Ion composition and dynamics at comet Halley

H. Balsiger*, K. Altwegg*, F. Bühler*, J. Geiss*, A. G. Ghielmetti†, B. E. Goldstein‡, R. Goldstein‡, W. T. Huntress‡, W.-H. Ip§, A. J. Lazarus‖, A. Meier*, M. Neugebauer‡, U. Rettenmund*, H. Rosenbauer§, R. Schwenn§, R. D. Sharp†, E. G. Shelley†, E. Ungstrup¶ & D. T. Young#

* Physikalisches Institut, University of Bern, 3012 Bern, Switzerland
† Lockheed Palo Alto Research Laboratory, Palo Alto, California 94304, USA
‡ Jet Propulsion Laboratory, Pasadena, California 91109, USA
§ Max-Planck-Institut für Aeronomie, D-3411 Katlenburg-Lindau, FRG
‖ Massachusetts Institute of Technology, Cambridge, Massachusetts 02139, USA
¶ Danish Space Research Institute, 2800 Lyngby, Denmark
# Los Alamos National Laboratory, Los Alamos, New Mexico 87545, USA

The ion mass spectrometer aboard the Giotto spacecraft measured the composition and velocity distributions of cometary ions at distances of $\sim 7.5\times10^6$ to $\sim$1,300 km from the nucleus of comet Halley. Well outside the bow shock, pick-up cometary H^+ ions were found in a diffuse shell-like distribution. Heavier ions (C^+, H_2O^+-group, CO^+ and S^+) with similar distributions have been identified at $\leq 3\times10^5$ km. Solar-wind He^{2+} was found throughout the coma to as close as $\sim$5,000 km; He^+ produced by charge exchange was seen inside $\sim 2\times10^5$ km. Deeper within the coma the main cometary hot-ion species identified were H^+, H_2^+, C^+, O^+, OH^+, H_2O^+, H_3O^+, CO^+ and S^+. A pile-up of heavy cometary ions was found at $\sim 10^4$ km from the nucleus. Giotto crossed the contact surface at $\sim$4,600 km, based on changes in ion flow velocity and temperature. Inside, ion temperatures as low as $\sim$340 K and outflow velocities of $\sim$1 km s^{-1} were found. Outside the contact surface ion densities vary as r^{-2}, with a transition to an r^{-1} dependence approximately at the contact surface. A large C^+ abundance throughout the coma indicates an unexpected direct source of atomic carbon. The nitrogen abundance, on the other hand, is relatively low.

The Giotto ion mass spectrometer (IMS) consists of two independent sensors: the high-energy-range spectrometer (HERS), which is optimized primarily for the study of ion abundances and velocity distributions outside the contact surface (CS); and the high-intensity spectrometer (HIS), which provides similar information primarily inside the CS. Both sensors returned complementary data of excellent quality throughout the encounter to within a few seconds of closest approach (CA), after which only the HIS returned data. We have reported elsewhere on the optical principles of the IMS and on its flight configuration and initial in-flight calibration[1]. The HERS and the HIS are true mass spectrometers using variable electric fields and static magnetic fields for simultaneous determination of energy per charge (E/Q), mass per charge (M/Q) and velocity distributions. The HERS E/Q range is 10 to 4,500 eV/e, depending on mass and including typical solar-wind energies. The HIS range is 300 to 1,400 eV/e. Both instrument fields of view are fans which rotate with the spinning spacecraft. Fan angles (called elevation angles) relative to the spin axis are +15° to +75° for the HERS (thus excluding the ram direction but including the solar-wind direction) and −3° to +12° for the HIS. Times to collect a full mass spectrum, including angular and energy information, are 16 s and 4 s for HERS and HIS, respectively.

Although calibration and background factors have been applied where indicated, the data must still be considered in some sense preliminary. A common system of coordinates and nomenclature has not yet been established by the Giotto experimenters, so here we refer to ground-station received time (in UT) and convert this to distance from the nucleus based on CA = 605 km on 14 March, 00:11:00 UT.

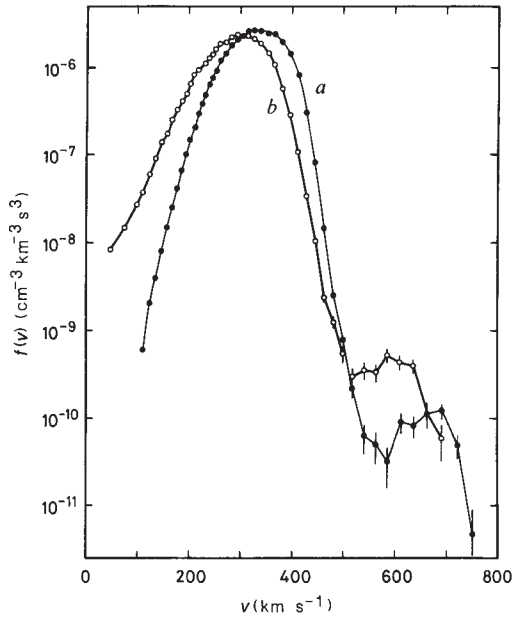

Fig. 1 The distributions of proton velocities parallel to the solar-wind velocity vector for two intervals before Giotto crossed the cometary bow shock. *a*: 13 March, 14:49–15:42 UT; proton speed, proton density and thermal Mach number: 334 km s^{-1}, 5 cm^{-3}, 5.5. *b*: 13 March, 19:03–19:27; solar wind parameters: 284 km s^{-1}, 6 cm^{-3}, 4.3. The thermal Mach number is defined as v/w, where v is the solar-wind velocity and the thermal speed $w=(2kT/M)^{1/2}$, where M is the proton mass.

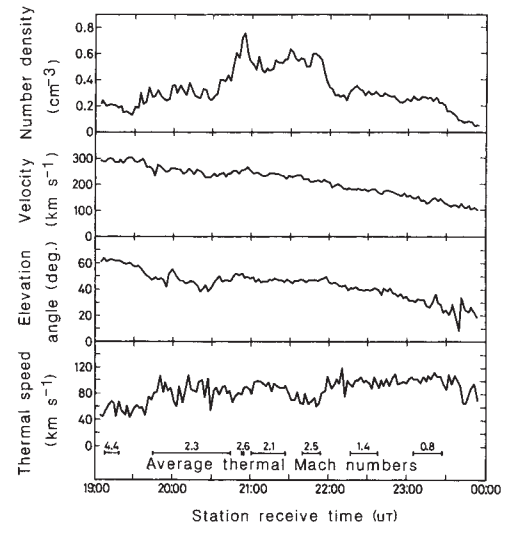

Fig. 2 Plasma parameters for the $M/Q=2$ ions, based on moments calculated from preliminary data. All plotted parameters are relative to the spacecraft reference frame, whereas the spacecraft velocity has been removed for calculation of the average thermal Mach numbers given below the plotted data. The elevation angle is measured from the spacecraft velocity vector; the solar direction has an elevation angle of 72.5°.

Plasma dynamics of solar-wind interaction. Pick-up protons of cometary origin first became noticeable in 53-min averages of the HERS proton-mode data at ~18:00 UT on 12 March (~7.5 × 10^6 km from the nucleus). Figure 1 shows two proton velocity spectra measured on 13 March in a 22° (azimuth) by 15° (elevation) angular sector which included the direction to the Sun.

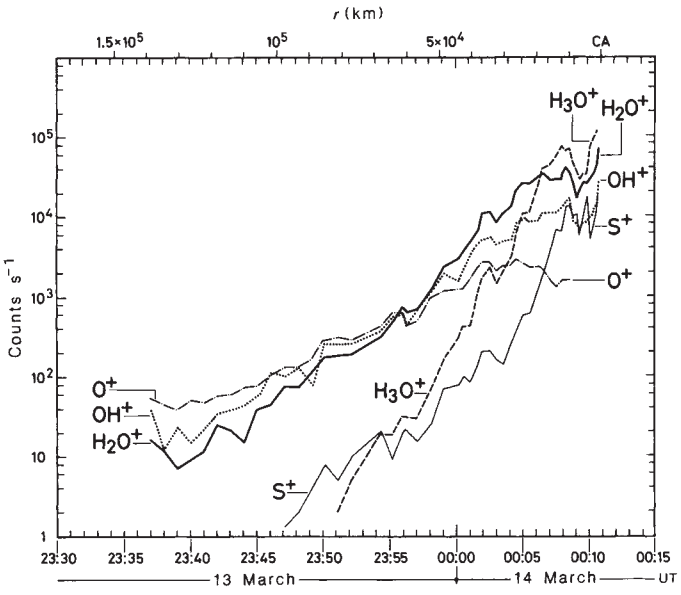

Fig. 3 Time profiles of the HIS count rates for masses 16, 17, 18 and 19 as well as the mass 32–34 group. Time is ground-station received time in UT; *r*, distance of Giotto from the nucleus.

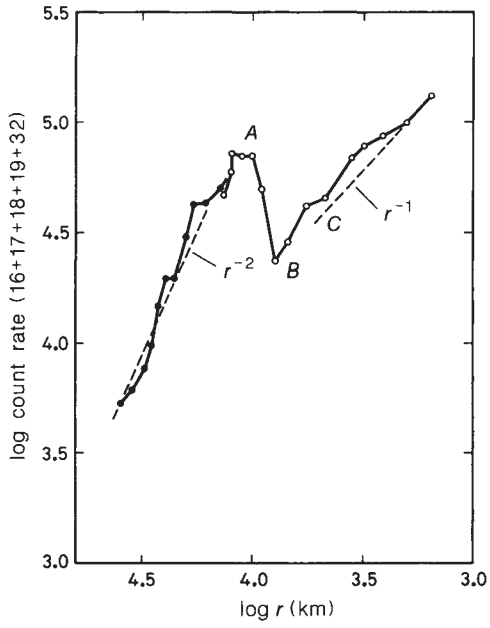

Fig. 4 Radial profile of the sum of the HIS count rates for masses 16, 17, 18, 19 and 32, showing that inside the 'contact surface' (*C*, at $r \simeq 4{,}600$ km) the total count rate tends to follow an r^{-1} dependence and that in the outer part ($r > 16{,}000$ km) an r^{-2} dependence fits the data quite well. Open circles, H-mode data; dots, N-mode data (see ref. 1).

Spectrum *a* was obtained at a distance of $\sim 2.2 \times 10^6$ km, and spectrum *b* at a distance of $\sim 1.2 \times 10^6$ km during the half-hour preceding the bow-shock crossing. Both spectra show secondary peaks at twice the solar-wind speed. This spectral shape is quite different from the power-law spectrum derived for water-group ions picked up near comet Giacobini-Zinner[2]. Examination of three-dimensional data obtained over the 360° × 60° field of view of the HERS instrument reveals that these picked-up protons were distributed over a spherical shell in phase space; this shell was centred on the solar-wind bulk velocity and had a radius equal to the solar-wind speed. Such a distribution function is consistent with rapid pitch-angle scattering of newly ionized hydrogen out of the expected initial cycloidal trajectories.

The features of spectra *a* and *b* listed in Fig. 1 legend illustrate that as Giotto approached the comet, the solar wind became slower, denser and hotter, as expected from models of the mass loading of the solar wind by photoionization of cometary gases[3–5]. As the mass loading proceeded, the relative number of protons in the shell increased from 0.2% of all protons in spectrum *a* to 0.7% in spectrum *b*. Clearly, most of the deceleration must have been caused by the pick-up of ions heavier than protons (see ref. 6, which describes the results of the implanted ion sensor).

The ions detected by HERS at $M/Q = 2$ AMU/e provide a good tracer for plasma variations associated with the comet–solar wind interaction because that M/Q value is expected to be populated primarily by solar-wind alpha particles until very close to the comet where cometary H_2^+ becomes an important constituent. Preliminary estimates of plasma parameters were obtained by taking moments of the $M/Q = 2$ distributions after subtracting the estimated background count rates. No adjustments were made for the part of the particle beam outside the HERS field of view; such corrections can be substantial when the beam is incident at elevation angles near 15° or 75°.

Figure 2 shows 128-s averages of the resulting parameters as measured in the spacecraft frame of reference, as functions of time. A weak but definite bow-shock-like transition was observed shortly after 19:30 UT at $\sim 1.15 \times 10^6$ km from the nucleus. The bulk speed decreased, number density and thermal speed increased, and the flow angle changed by ~10°, rotating away from the Sun–comet line. The average thermal Mach number dropped from 4.4 before to 2.3 after the shock. The protons underwent equivalent changes, and the highest-time-resolution proton data (1 spectrum every 16 s) suggest multiple crossings of the shock between 19:30 and 19:39 UT. The identification of a bow shock close to the theoretically expected location is one clear difference from the plasma observations at comet Giacobini-Zinner[7].

After the shock, there is a roughly steady decrease in speed and in apparent elevation angle. When the effect of the spacecraft velocity is removed, it is seen that the plasma speed decreased rather steadily from ~300 to < 100 km s^{-1} between 19:40 UT (1.1×10^6 km) and 23:40 UT (1.2×10^5 km), while the flow direction fluctuated between 20° and 40° away from the Sun–comet line. The density and thermal speed (and the thermal Mach number) showed a more structured radial profile through this region. From ~20:45 to 21:55 UT the density was greater by a factor of ~2, while the flow direction shifted back to a more nearly anti-sunward direction. During the same period the magnetometer observed a considerably quieter field than during the preceding hour[8]. This high-density structure may have been caused by temporal variation in either the solar wind or the gas emitted from the comet.

Following the region of high density, the speed continued to decrease, causing the apparent flow direction to turn more towards the ram direction. After ~22:00 UT, the $M/Q = 2$ ions developed a very non-thermal distribution, suggestive of the presence of H_2^+ ions in addition to He^{2+} (see below), and by the end of the day, 25–50% of the $M/Q = 2$ ions had dropped out of the HERS field of view. At 23:40 UT there was a very large fluctuation in the plasma flow direction.

Plasma dynamics of coma ions. Between ~22:00 and ~23:53 UT (5.4×10^5 to 7.4×10^4 km), HERS detected an increasing flux of hot cometary ions; the mass spectra of these ions are described below. Then, beginning at ~23:53 UT, the ion fluxes seen by HERS decreased while the HIS ion count rates increased. Figure 3 shows HIS count rate profiles for several ion species. By ~00:05:30 (22,500 km), the ion population was so stagnant and cold that the HERS count rates were down to background levels (except for the protons, which decreased in count rate, but did not disappear). We attribute this strong cooling of the solar-

wind ion component to charge exchange and collisional effects. The distribution of cometary ions in this collision-dominated region was, however, still significantly affected by the solar-wind flow; this is demonstrated by the steeper than r^{-1} dependence of the HIS count rates at radial distances $>10^4$ km. In Fig. 4 we show that an r^{-2} dependence fits the data quite well. At point C (Figs 4 and 5), 4,600 km from the nucleus, we identify a clear discontinuity in ion velocity and temperature, which we call the 'contact surface' (see Fig. 5). At the same location the magnetic field strength dropped to zero[8]. The r^{-1} dependence of the count rate inside such a diamagnetic cavity has been predicted by photochemical equilibrium models in which the photoionization of cometary neutrals is balanced by electron dissociative recombination in a spherically symmetric coma.

One of the distinct features of the ion profile is the apparent pile-up of heavy ions just outside 10^4 km from the nucleus (A in Fig. 4) and the subsequent minimum (B). The discontinuity in the count rates between A and B is not yet well understood. Several effects could be involved here. First, the coma outside the contact surface confining the ionospheric outflow may be permeated by a flux of ionizing electrons: these electrons would not only produce additional ions but due to their much higher temperature the electron recombination loss would be reduced, thus producing enhanced ion concentration. Second, the possibility of plasma transport along the draped field lines in the 'magnetosheath' could produce the minimum in region B (ref. 4). Finally, the observed structure may be simply temporal, reflecting a change in the solar-wind condition and/or in the outgassing of the comet.

A major function of the HIS instrument was to measure the velocity distribution function for different ion species in the cometary ionosphere. Fig. 5 shows the time profiles of the flow speeds determined from the mass 18 (H_2O^+) and 19 (H_3O^+) ions (after subtraction of the spacecraft speed), as well as the corresponding temperatures (T_i). Although further analysis will be required to clarify the several fine-scale structures, the general trend of larger flow speeds and temperatures at larger distances from the cometary nucleus is obvious. Also, the drastic change in ion temperature at ~00:09:54 UT, from 2,600 to ≤450 K, is quite striking. The drop in temperature coincides with a sudden onset of a ~1 km s^{-1} flow velocity outwards from the comet. As mentioned, we call this discontinuity the 'contact surface'. The measured outflow speed for the ionospheric plasma is in general agreement with theoretical calculations; the low temperature of the water-group ions inside the contact surface can be understood in terms of a balance between photolytic heating of the expanding ionospheric plasma and the very efficient cooling effect of collisions with H_2O molecules[9].

Ion composition from HERS mass spectra. Figure 6 shows relative M/Q count-rate spectra acquired in three radial intervals, indicated in the legend. Examination of the three-dimensional velocity distributions of all of the prominent ion constituents observed in the medium (M-mode; $M/Q = 12$–26) and heavy (H-mode; $M/Q = 15$–34) mass modes showed that they were very nearly identical. The spectra shown are averaged over the full width at half-maximum of these distributions.

The M/Q peaks shown in Fig. 6 are derived from laboratory calibrations; the identification of specific ion species associated with the M/Q measurements is discussed below. The transformation from ion count rate to density is dependent on mass, energy and elevation angle, but to a rough approximation the count rates are proportional to phase-space density divided by $(M/Q)^4$. This relationship has been confirmed by performing the detailed transformation for a limited number of cases and the results are shown in Table 1.

Figure 7 shows light-ion (L-mode) spectra recorded at two radial distances. Figure 7*a*, from 2.5–3.2 × 10^5 km, is characteristic for a region inside the bow wave which is still dominated by solar-wind ions. Mass peaks are shown for He^{2+}, O^{7+}, O^{6+} and C^{5+}, which are typically identified in solar-wind spectra[10].

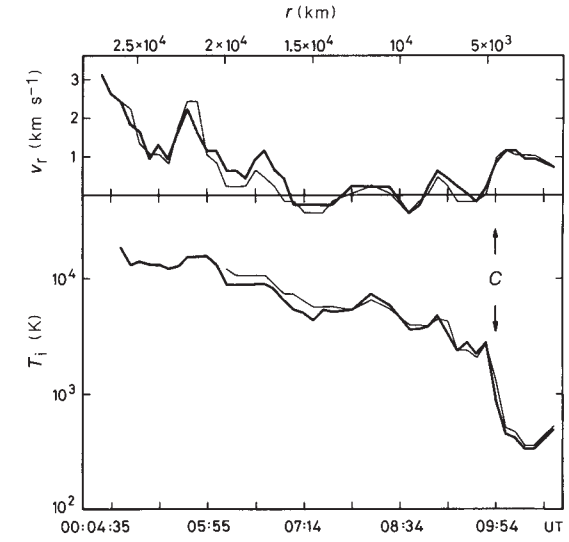

Fig. 5 Time profiles of the ionospheric flow speed relative to the comet (v_r) and temperature (T_i) derived from an analysis of the HIS count rates of mass 18 (H_2O^+; bold line) and 19 (H_3O^+; thin line). Note that v_r changes from near-zero to ~1 km s^{-1} at the contact surface (C). At the same location, T_i decreases rapidly from 2,600 to ≤450 K.

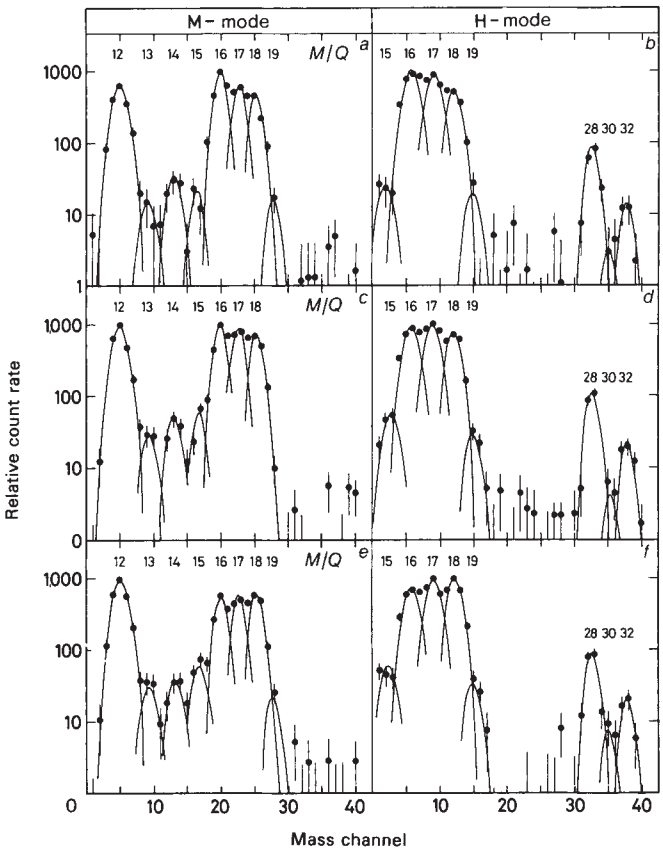

Fig. 6 M/Q spectra acquired by HERS in three radial intervals. *a*, *b*: 13 March, 23:25–23:44 UT; $r = 1.1$–1.7×10^5 km. *c*, *d*: 13 March, 23:54 UT; $r = 0.7$–1.1×10^5 km. *e*, *f*: 13/14 March, 23:53–00:02 UT; $r = 3.5$–7.0×10^4 km. Error bars indicate one standard deviation based on counting statistics only. To a rough approximation, count rates are proportional to relative phase-space densities divided by $(M/Q)^4$. M/Q peaks are shown to indicate the response to specific mass components.

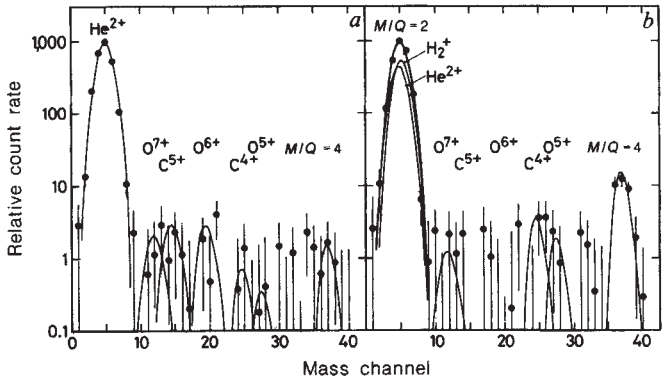

Fig. 7 Light-ion mass spectra from HERS in, *a*, the outer coma (13 March, 22:54–23:10 UT; $r = 2.5$–3.2×10^5 km), indicating primarily unaltered solar-wind composition and, *b*, deeper in the coma (13/14 March, 23:44–00:03 UT, $r = 0.3$–1.1×10^5 km), showing a mixture of partially charge-exchanged solar-wind ions (in particular He^+) and cometary hydrogen, H_2^+.

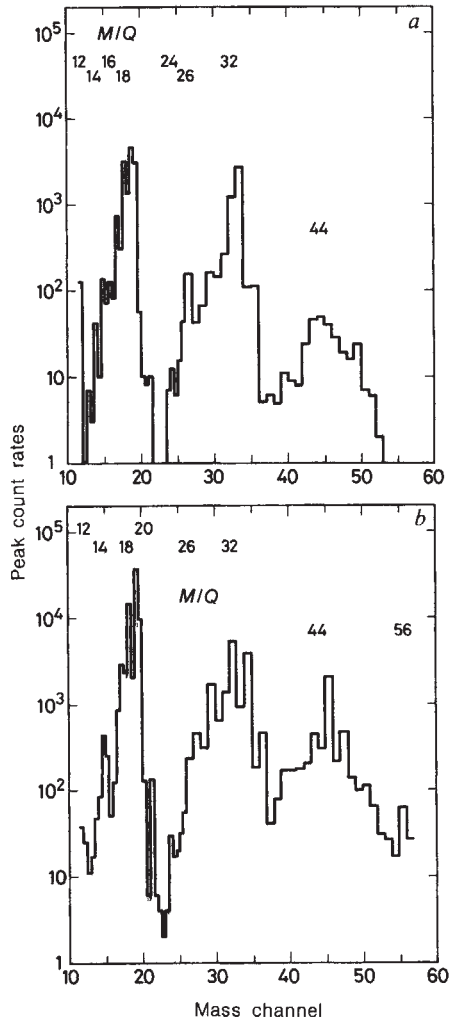

Fig. 8 Peak count rates from HIS in H-mode (see ref. 1) obtained in one spin. *a*: 14 March, 00:09:32 UT; $r \simeq 6{,}000$ km (outside the contact surface). *b*: 14 March, 00:10:42; $r \simeq 1{,}500$ km (inside the contact surface). Note that mass channels are not identical with M/Q.

There is some evidence for peaks at $M/Q = 3$ (C^{4+}), 3.2 (O^{5+}) and 4. These latter appear more clearly in the inner region (Fig. 7*b*, from 0.3–1.1×10^5 km), which is dominated by cometary ions (see Fig. 6*c*–*f*) and charge-exchanged solar-wind ions. Here we identify a major contribution of cometary H_2^+ to the $M/Q = 2$ peak. From the $M/Q = 4$ peak we infer that ~30% of solar-wind helium has charge-exchanged to He^+. The $M/Q = 3$ peak could contain cometary H_3^+ in addition to the solar-wind C^{4+}.

After count rates in HERS had dropped to background level (by ~00:05:30 UT), a flux of hot ions abruptly reappeared approximately at or inside the contact surface (~4,600 km). The last data transmission received from HERS (00:10:36 UT) indicated instantaneous H-mode ($M/Q = 15$–34) count rates higher than at any other time during the inbound pass of Giotto. The ions showed quite low bulk speed (equal to or less than the ram velocity), with a thermal distribution corresponding to a Mach number of ~1. They were of mainly cometary origin, quite similar to the composition observed by HERS further out. The $M/Q = 2$ peak was identified as mainly cometary H_2^+. More extensive analysis, including the investigation of possible influence from dust impact and spacecraft charging shortly before closest approach, will be required to understand these data in more detail.

Ion composition from HIS mass spectra. HIS observed ion spectra from ~2×10^5 km through closest approach. It was operated in two different modes, called N and H (ref. 1). Figure 8 shows two spectra from the H-mode. More detailed analysis and inclusion of both modes will eventually lead to relative ion densities and spectra better resolved than those shown here. Nonetheless, a number of important observations regarding species identification can be readily made. There are three prominent groups of ions seen in Fig. 8. The most abundant is the water group at $M/Q = 17$–19. The pattern exhibited by the ion group $M/Q = 13$–16 is characteristic of methane, with some contribution at $M/Q = 16$ from O^+. Although the instrument sensitivity is significantly reduced at $M/Q = 12$, a relatively large peak is observed from C^+. The second group of ions at $M/Q = 24$–34 is the region in which CO^+, HCN^+, H_2S^+, $C_2H_n^+$ hydrocarbons, single-carbon organics and sulphur contribute. This second group is dominated at distances >4,000 km by the S^+ ion ($M/Q = 32$). The third group of ions at $M/Q = 36$–54 is the region in which CO_2^+, the $C_3H_n^+$ and $C_4H_n^+$ hydrocarbons, other two- and three-carbon organics and sulphur species such as CS^+ and SO^+ contribute. Chemical modelling will be required to provide specific identifications in the second and third groups.

A comparison of the two mass spectra (Fig. 8*a*, *b*), one taken at 6,000 km and the other at 1,500 km, indicates substantial changes in ion composition as a function of the radial distance. The increase in the count rates of species other than the H_2O^+-, CO^+-, S^+- and CO_2^+-group ions at smaller distances to the nucleus is particularly noteworthy; this suggests a significant contribution of hydrocarbons and carbon organics to the ion chemistry in the inner coma.

More thorough analysis of the innermost spectra should also lead to the resolution of the $M/Q = 20$ ($H_2D^{16}O^+ + H_3{}^{17}O^+ + H_2{}^{18}O^+$) and 21 (mainly $H_3{}^{18}O^+$) peaks from the main water-group peaks 17 ($^{16}OH^+$), 18 (mainly $H_2{}^{16}O^+$) and 19 (mainly $H_3{}^{16}O^+$) and thus give us the opportunity to deduce the D/H ratio in cometary water.

Ion chemistry. Outside the contact surface, at distances from the nucleus of 0.35–1.7×10^5 km, the most abundant ions are O^+ at $M/Q = 16$, OH^+ at $M/Q = 17$, and H_2O^+ at $M/Q = 18$. The relative count rates at $M/Q = 16$–18 versus cometary distance (see Fig. 3) are consistent with the successive photodissociation of water to OH and O followed by photoionization of each component. There is some contribution at $M/Q = 17$ from dissociative photoionization of H_2O to OH^+. At these distances from the nucleus, ion–molecule reactions in the coma are not important and the count rate at $M/Q = 19$ (H_3O^+) is low.

The C^+ ion at $M/Q = 12$ has an unexpectedly high abundance. The intensity at $M/Q = 13$ is too large for this ion to be due to the ^{13}C isotope alone: the main contributor to $M/Q = 13$ is the CH^+ ion. Assuming that CH^+, CH_2^+ and CH_3^+ are the major contributors to $M/Q = 13$–15, and considering the respective photodissociation and ionization rates, a mixture of 2–7% methane in water fits the ion intensity distribution fairly well, including the variation with radial distance out to $\sim 10^5$ km. At greater distances there may be a contribution at $M/Q = 14$ from N^+ ions. At this early stage in the data analysis, we find no definite evidence for the presence of NH_3 in the ion mass spectra.

In the outer coma the major ions in the spectrum beyond $M/Q = 19$ are CO^+ at $H/Q = 28$, S^+ at $M/Q = 32$ and CO_2^+ at $M/Q = 44$. The ion at $M/Q = 28$ is most likely the CO^+ ion rather than N_2^+. An upper limit for the contribution of the N_2^+ ion to $M/Q = 28$ can be deduced by using the $M/Q = 14$ peak in the HERS spectrum at $1.1 - 1.7 \times 10^5$ km (Fig. 6*a*, *b*) to derive the required $M/Q = 28$ intensity. In this particular spectrum, N_2^+ can contribute no more than 10% to the total $M/Q = 28$ intensity.

The S^+ ions arise from the photoionization of S atoms, which are in turn the result of the photodissociation of CS, S_2, CS_2, H_2S and other sulphur-containing species. The ultraviolet emissions of the first two species have been seen in several comets by the International Ultraviolet Explorer spacecraft[11,12]. The relative count rates of the S^+ ions and the H_2O-group ions suggests that the production rate of the sulphur-containing parent molecules is $\sim 10^{-3}$ times that of the water molecules. The S^+ count rate, however, increases to $\sim 10\%$ that of the H_3O^+ ions at $\sim 1{,}500$ km (Fig. 8*b*). This enhancement can be explained by the shorter photoionization timescale and much longer electron radiative recombination time for S^+ ions as compared with water ions[13].

In view of the possible identification of Na^+ and/or Mg^+ ions in the ion tail of comet Giacobini-Zinner[14], a surprise in the Halley encounter observations is the near-absence of Na^+ ions (Fig. 8). The peak at $M/Q = 56$ in Fig. 8*b* persists in several measurements and may possibly be the Fe^+ ion.

Inside $\sim 2 \times 10^4$ km, the dominance of H_3O^+ demonstrates the importance of ion–molecule reactions. The dominance of H_3O^+ also requires that the abundance of NH_3 be less than $\sim 3\%$ that of H_2O[13,15]. The peaks at $M/Q = 28$ and 29 which would be expected from CO^+ and HCO^+ are less significant inside the contact surface because of the high reactivity of these ions towards H_2O. The same holds true for CO_2^+ and HCO_2^+ ions at $M/Q = 44$ and 45. The relative intensities of ions with $M/Q = 28$ and 44 outside the contact surface indicate that there is somewhat less CO_2^+ than CO^+. There are also significant numbers of ions present in the spectrum at $M/Q = 24$–27, where C_2H_2 and HCN contribute.

A major surprise in the HERS data is the very large signal from the C^+ ion at $M/Q = 12$. Dissociative photoionization of CO, CH_4 and CO_2, and photodissociation of CO, CH_4 and CO_2 to C followed by photoionization of C, together cannot account for all of the C^+ ions in the HERS mass spectrum. The simplest explanation is that the $M/Q = 12$ peak arises from atomic carbon. If expressed as atomic carbon, this component of the cometary gas would be 5–10% of the total number of oxygen atoms at these distances. HIS, although providing only a lower limit for C^+, also indicates a large abundance of C^+ at all distances. Either there is an additional, hitherto unexpected ionization mechanism leading selectively to C^+, or there is an unexpected source of atomic carbon in the coma of comet Halley. Carbon atoms might be released directly at the surface, or the source may be the dust grains themselves. Carbonaceous grains in the coma may be stimulated by solar ultraviolet photons to release carbon in atomic form, or as a highly unsaturated compound. Small carbonaceous dust grains as observed by the Giotto particle impact analyser[16] will have a high temperature in the coma[17] and slow outgassing could provide a distributed source of some material readily photolysed to atomic carbon.

While the IMS spectra show a striking richness in carbon they also show a noticeable lack of nitrogen. Using the HERS ion densities from Table 1 at the range 0.70–1.1×10^5 km, we find a bulk C/O ratio of 0.33, an upper limit to the N/O ratio of ≤ 0.01 and an S/O ratio of 0.03. The C/O ratio is about half the cosmic ratio, the N/O ratio is low by an order of magnitude, and the S/O ratio is cosmic.

Table 1 HERS preliminary ion number densities (cm^{-3})

Range ($\times 10^5$ km)	$M/Q = 12$	16	17	18	28	32
0.35–0.70	3.4	5.6	8.6	11	6.1	
0.70–1.1	5.3	16	18	18	14	5.9
1.1–1.7	2.6	11	8.8	6.9	6.2	

The rather high abundance for CO that would be derived from the ratio of $M/Q = 28$ to water-group ion densities in Table 1 ($CO/H_2O \simeq 0.2$) is only an upper limit because this CO represents all carbonaceous gas-phase species processed by photochemistry in the coma to CO.

We acknowledge the dedicated support of the many technicians in ESA and at our institutes who made this experiment possible. We are grateful to R. G. Johnson and H. Bridge for important contributions to the IMS team and we thank K. Bratschi and R. Wright for graphics and T. Feller for typing. This work was supported by NASA, the German Bundesministerium für Forschung und Technologie and the Swiss National Science Foundation.

Received 14 April; accepted 23 April 1986.

1. Balsiger, H. *et al. Eur. Space. Ag. spec. Publ.* **1077,** 129–148 (1986).
2. Gloeckler, G. *et al. Geophys. Res. Lett.* **13,** 251–254 (1986).
3. Bierman, L., Brosowski, B. & Schmidt, H. U. *Sol. Phys.* **1,** 254–284 (1967).
4. Ip, W. H. & Axford, W. I. in *Comets* (ed. Wilkening, L. L.) 588–634 (University of Arizona Press, Tucson, 1982).
5. Schmidt, H. U. & Wegmann, R. in *Comets* (ed. Wilkening, L. L.) 538–560 (University of Arizona Press, Tuscon, 1982).
6. Johnstone, A. *et al. Nature* **321,** 344–347 (1986).
7. Bame, S. J. *et al. Science* **232,** 356–361 (1986).
8. Neubauer, F. *et al. Nature* **321,** 352–355 (1986).
9. Shimizu, M. *Astrophys. Space Sci.* **40,** 149–155 (1976).
10. Kunz, S. *et al. Sol. Phys.* **88,** 359–376 (1983).
11. Feldman, P, D. in *Comets* (ed. Wilkening, L. L.) 461–479 (University of Arizona Press, Tucson, 1982).
12. A'Hearn, M. F., Feldman, P. D. & Schleicher, D. G. *Astrophys. J.* **274,** L99–L103 (1983).
13. Aikin, A. C. *Astrophys. J.* **193,** 263–264 (1974).
14. Ogilvie, K. W., Coplan, M. A., Bochsler, P. & Geiss, J. *Science* (in the press).
15. Ip, W.-H. *Eur. Space Ag. spec. Publ.* **169,** 79–91 (1981).
16. Kissel, J. *et al. Nature* **321,** 336–337 (1986).
17. Hanner, M. S. in *Cometary Exploration* Vol. 2 (ed. Gombosi, T. I.) 1–22 (Central Research Institute for Physics, Budapest, 1982).